Delivery of pollutants by spawning salmon

Fish dump toxic industrial compounds in Alaskan lakes on their return from the ocean.

Pollutants are widely distributed by the atmosphere and the oceans[1]. Contaminants can also be transported by salmon and amplified through the food chain. Here we show that groups of migrating sockeye salmon (*Oncorhynchus nerka*) can act as bulk-transport vectors of persistent industrial pollutants known as polychlorinated biphenyls (PCBs), which they assimilate from the ocean and then convey over vast distances back to their natal spawning lakes. After spawning, the fish die in their thousands — delivering their toxic cargo to the lake sediment and increasing its PCB content by more than sevenfold when the density of returning salmon is high.

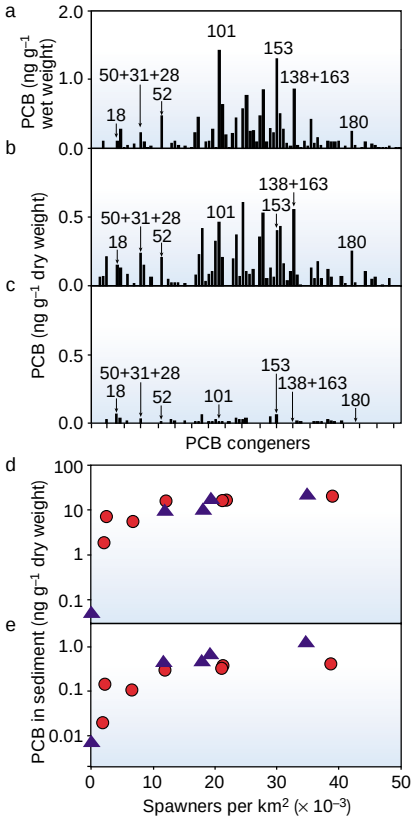

Figure 2 Surface sediments in Alaskan lakes show a similar pattern of polychlorinated biphenyl (PCB) congeners to that found in salmon returning to spawn, and sedimentary PCB concentrations are strongly correlated with the density of salmon returning. **a–c,** PCB congener patterns (numbers represent different congeners) in **a,** sockeye salmon from Frazer Lake; **b,** surface sediments from Frazer Lake (total escapement, about 11,700 spawners per km^2); and **c,** surface sediments from Spiridon Lake (no anadromous salmon return). The standard deviation for salmon densities over the past ten years was on average about 50% of the mean for each lake. **d, e,** PCB concentrations in lake-surface sediment are shown as a function of salmon escapement density as the sum of 127 PCB congeners (**d**) and as the single PCB congener 101 (**e**). Resampling in 2002 (triangles) confirmed the 1995–1998 data (circles). Further methodological details are available from the authors.

Sockeye salmon spawn in freshwater after spending most of their life in the ocean, and die after spawning. They acquire more than 95% of their biomass in the north Pacific Ocean[2,3] and then return to their nursery lakes, which may be more than 1,000 km from the ocean[4]. The lipids accumulated by salmon to fuel this long upstream migration sequester PCB compounds: from a PCB concentration of less than 1 ng per litre in the ocean[5,6], sockeye salmon accumulate PCBs to a concentration of 2,500 ng per gram of lipid[7]. This means that one million adult salmon could transport more than 0.16 kg of PCBs to the spawning area, which is comparable to the amount of fugitive PCBs released annually from hazardous waste incinerators[8]. Fat-soluble PCBs are transported to freshwaters, where they enter aquatic and terrestrial foodwebs[7].

During 1995, 1997, 1998 and 2002, we collected sediment cores from eight lakes, providing a range of salmon-return densities from 0 to 40,000 spawners per km^2 (Fig. 1). Surface sediments (0–2 cm in thickness), representing the past 5.3 ± 3.5 years of accumulation on the basis of our calculated sedimentation rates, were extracted for PCB analysis. We also measured PCB concentrations in muscle tissue of sockeye salmon ($n = 5$) to identify the signature of the source (Fig. 2a).

Surface sediments of Frazer Lake (which has annual salmon returns of 11,700 fish per km^2) show patterns and concentrations of the most abundant PCBs that are similar to those carried by spawning sockeye returning to that lake (Fig. 2b). In particular, the PCB congeners designated as 101, 118, 153 and 138 + 163 were among the most abundant in both sockeye salmon and Frazer Lake sediments. More telling are the concentrations and patterns in Spiridon Lake, which receives no salmon spawners (Fig. 2c). Concentrations of PCBs in sediments from this lake are tenfold lower, and include a greater proportion of lighter congeners, which are effectively transported by air[9].

The PCB concentration and accumulation rate in sediment correlate strongly with the density of salmon returning ($r^2 > 0.9$; Fig. 2d, e). For example, lakes with annual salmon returns of fewer than 5,000 spawners per km^2 contained accumulated PCB concentrations of less than 2 ng g^{-1} (or less than 500 ng m^{-2} yr^{-1}) in their surface sediments, compared with about 20 ng g^{-1} (or about 3,700 ng m^{-2} yr^{-1}) for the lake with the highest density of returning salmon (40,000 spawners per km^2).

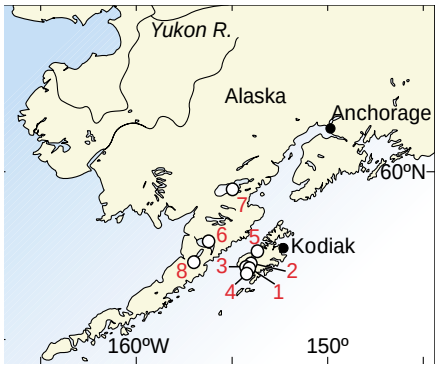

Figure 1 Location of the eight lakes where surface sediments and sockeye salmon were collected: 1, Frazer; 2, Karluk; 3, Red; 4, Olga; 5, Spiridon; 6, Becharof; 7, Iliamna; 8, Ugashik.

Lakes with the highest densities of spawning salmon would contribute 0.12 kg fish biomass per m^2, or 6,000 ng PCB m^{-2} yr^{-1}. Some PCB might be lost by degradation and recycling to the water column. These values may be compared with a background PCB accumulation of about 1,000 ng m^{-2} yr^{-1} for 11 lakes distributed from mid-latitudes up to the Arctic in Canada[9]. The transport of PCBs by 40,000 salmon per km^2 could therefore result in a roughly sixfold increase above atmospheric loading in a remote setting, a prediction that compares well with our observations (Fig. 2d, e).

The amount of PCBs transported by sockeye salmon to these lakes is greater than the traditional assignment from atmospheric pathways. Returning sockeye salmon act as 'biological pumps' by transporting contaminants upstream, where pollutants may affect their offspring and/or predators such as bears, eagles and humans. Whether these contaminants affect juvenile salmon survival is as yet unknown, but they are suspected of causing immunosuppression[10]. Ironically, the marine-nutrient pump, which historically has increased successful recruitment, may now pose a risk to some of these populations.

E. M. Krümmel*, R. W. Macdonald†, L. E. Kimpe*, I. Gregory-Eaves*, M. J. Demers*, J. P. Smol‡, B. Finney§, J. M. Blais*

**Department of Biology, University of Ottawa, Ottawa, Ontario K1N 6N5, Canada*
e-mail: jblais@science.uottawa.ca
†Institute of Ocean Sciences, Department of Fisheries and Oceans, Sidney, British Columbia V8L 4B2, Canada
‡Paleoecological Environmental Assessment and Research Laboratory, Department of Biology, Queen's University, Kingston, Ontario K7L 3N6, Canada
§Institute of Marine Science, University of Alaska

Fairbanks, Fairbanks, Alaska 99775, USA

1. Macdonald, R.W. *et al. Sci. Total Environ.* **254,** 93–234 (2000).
2. Finney, B. P., Gregory-Eaves, I., Sweetman, J., Douglas, M. S. & Smol, J. P. *Science* **290,** 795–799 (2000).
3. Naiman, R. J. *et al. Ecosystems* **5,** 399–417 (2002).
4. Burgner, R. L. in *Pacific Salmon Life Histories* (eds Groot, C. & Margolis, L.) 1–117 (UBC, Vancouver, 1991).
5. Iwata, H. *et al. Environ. Sci. Technol.* **27,** 1080–1098 (1993).
6. Indian and Northern Affairs *Canadian Arctic Contaminant Assessment Report: Sources, Occurrence, Trends and Pathways in the Physical Environment* (Can. Ministry Pub. Works Govt Serv., Ottawa, 2003).
7. Ewald, G. *et al. Arctic* **51,** 40–47 (1998).
8. Blais, J. M. *et al. Environ. Toxicol. Chem.* **22,** 126–133 (2003).
9. Muir, D. C. G. *et al. Environ. Sci. Technol.* **30,** 3609–3617 (1996).
10. Arkoosh, M. R. *et al. J. Aquat. Anim. Health* **10,** 182–190 (1998).

Competing financial interests: declared none.

Kinematics

Wide shear zones in granular bulk flow

Granular matter does not flow homogeneously like a fluid when submitted to external stress, but usually forms rigid regions that are separated by narrow shear bands where the material yields and flows[1–13] (examples include geological faults[9–11], avalanches[12] and silo discharges[2,13]). Shear bands are narrow (five to ten grains in diameter[1–13]) and dependent on the particle shape[5], and often localize near a boundary[4–8,12,13]; they hinder mixing and make grain flows difficult to predict or describe[1–3]. Here we show that the shear zones created in the bulk of the material are wider than those near the walls, and that their bulk velocity profiles lie on a universal curve. This finding challenges the accepted picture of shear banding in granular media.

To create tunable shear zones away from lateral boundaries, we modified a Couette cell by splitting its bottom at radius R_s and attaching the two resulting concentric rings to the inner and outer cylinder (Fig.1a, b). The cell was filled with grains up to a height h, the outer cylinder and its co-moving ring were rotated, and the resulting flow was monitored from above by a fast CCD (charge-coupled-device) camera. We investigated the behaviour of many different types of grain, but only show results for spherical glass beads (diameter, 0.3 ± 0.1 mm).

The flow rapidly relaxed to a steady state, was purely azimuthal and was proportional to the driving rate, Ω (refs 4–8). We fixed Ω at 0.16 rad s^{-1} and measured $\omega(r)$, the dimensionless ratio of the average angular velocity, and Ω as a function of the radial coordinate. For shallow layers, a narrow shear zone developed above the split at R_s. When h was increased, this shear zone shifted away from R_s and broadened continuously and without any apparent boundary (Fig. 1b, c) — the widest zones exceeded 50 grain-diameters. The shear zone reached the inner cylinder and eventually localized there[5,7] when the height was sufficiently large. There was, however, a substantial range of layer heights where there were wide, symmetric bulk shear zones.

After appropriate rescaling, all of these bulk velocities collapse onto a universal curve, which is extremely well described by an error function ('erf'; Fig. 1d)

$$\omega(r) = 1/2 + 1/2\mathrm{erf}((r - R_c)/W) \qquad (1)$$

The strain rate is therefore gaussian, and the shear zones are completely determined by their centres, R_c, and widths, W. The fit to equation (1) is just as good for particles of different size and shape. Unlike shear bands localized at walls[5], bulk shear zones are universal — that is, they are not qualitatively influenced by the granular 'microstructure'. Removal of the inner cylinder while retaining the stationary bottom disc (dark green in Fig. 1a, b) does not affect the bulk profiles.

The evolution of the velocity profile from a step function at the bottom to an error function at the surface is reminiscent of a diffusive process along the vertical axis. However, W grows faster than $\sqrt{h}$, as diffusion would suggest, but slower than h. The shear zone's width is independent of R_s, but varies with particle size and type, hinting at a non-trivial internal length scale. By contrast, the location of the shear zone's centre, R_c, is particle-independent. Therefore, the only relevant length scales for R_c are h and R_s, and we find that the dimensionless displacement of the shear zone is well fitted by $(R_s - R_c)/R_s = (h/R_s)^{(5/2)}$.

Our results suggest that, for large R_s and h, the shear zones become arbitrarily broad. This raises the question of whether shear banding is intrinsic to granular matter or only occurs for particular flow geometries. Continuum theories, which should be able to describe granular shear zones, are severely constrained by the universality of the velocity profiles and the shear-zone positions, and should also incorporate the strong influence of the boundary. Our simple experimental protocol can be used to investigate unexpected regimes of granular flow, not least with a view to answering the basic question of how sand flows.

Denis Fenistein, Martin van Hecke

Kamerlingh Onnes Laboratory, Leiden University, 2300 RA Leiden, The Netherlands

e-mail: fenistein@phys.leidenuniv.nl

1. Duran, J. *Sand, Powders and Grains* (Eyrolles, Paris, 1997).
2. Nedderman, R. *Statics and Kinematics of Granular Materials* (Cambridge Univ. Press, Cambridge, 1992).
3. Jaeger, H. M., Nagel, S. R. & Behringer, R. P. *Rev. Mod. Phys.* **68,** 1259–1272 (1996).
4. Hartley, R. R. & Behringer, R. P. *Nature* **421,** 928–930 (2003).
5. Mueth, D. M. *et al. Nature* **406,** 385–389 (2000).
6. Howell, D. W., Behringer, R. P. & Veje, C. T. *Phys. Rev. Lett.* **82,** 5241–5244 (1999).
7. Losert, W., Bocquet, L., Lubensky, T. C. & Gollub, J. P. *Phys. Rev. Lett.* **85,** 1428–1431 (2000).
8. Lätzel, M., Luding, S., Herrmann, H. J., Howell, D. W. & Behringer, R. P. Preprint http://arxiv.org/abs/cond-mat/0211274
9. Scott, D. R. *Nature* **381,** 592–595 (1996).
10. Oda, M. & Kazama, H. *Géotechnique* **48,** 465–481 (1998).
11. Muhlhaus, H. B. & Vardoulakis, I. *Géotechnique* **37,** 271–283 (1987).
12. Daerr, A. & Douady, S. *Nature* **399,** 241–243 (1999).
13. Pouliquen, O. & Gutfraind, R. *Phys. Rev. E* **53,** 552–560 (1996).

Competing financial interests: declared none.

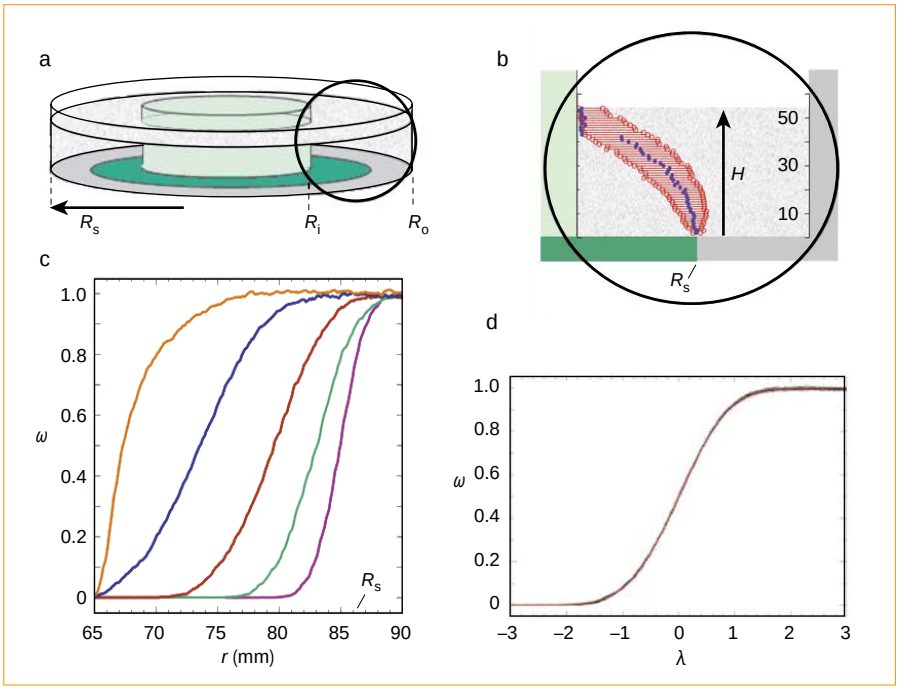

Figure 1 Creation of very wide shear zones in a flowing granular medium. **a,** Sketch of our split-bottomed Couette cell; stationary parts are shown in green. $R_i = 65$ mm, $R_0 = 105$ mm; R_s can be varied. **b,** Extension of the shear zone (circled in **a**), where the angular velocity, $\omega(r)$, ranges from 0.1 to 0.9 as a function of the level-height of the grains in the cell, h, for $R_s = 85$ mm. **c,** Velocity profiles showing the evolution of the ratio of the average angular velocity, $\omega(r)$, with h; values of h from left (in mm) are: 50, 40, 30, 20, 10. **d,** Universal bulk angular-velocity profiles obtained for different heights and plotted as a function of the rescaled radial coordinate $\lambda = (r - R_c)/W$. Red curve is an error function.